RESEARCH ARTICLE

JOURNAL OF
MEDICAL VIROLOGY WILEY

Type-II IFN inhibits SARS-CoV-2 replication in human lung epithelial cells and ex vivo human lung tissues through indoleamine 2,3-dioxygenase-mediated pathways

Dong Yang[1,2] | Jasper Fuk-Woo Chan[2,3,4,5,6,7,8] (ID) | Chaemin Yoon[2] | Tsz-Yat Luk[2] | Huiping Shuai[2] | Yuxin Hou[2] | Xiner Huang[2] (ID) | Bingjie Hu[2] | Yue Chai[2] | Terrence Tsz-Tai Yuen[2] | Yuanchen Liu[2] | Tianrenzheng Zhu[2] | Huan Liu[2] | Jialu Shi[2] | Yang Wang[2] | Yixin He[2] | Ko-Yung Sit[9] | Wing-Kuk Au[9] | Anna Jinxia Zhang[2,4] | Shuofeng Yuan[2,3,4] (ID) | Bao-Zhong Zhang[10] | Yao-Wei Huang[1] | Hin Chu[2,3,4]

[1]Xianghu Laboratory, Hangzhou, Zhejiang, China

[2]State Key Laboratory of Emerging Infectious Diseases, Department of Microbiology, School of Clinical Medicine, Carol Yu Centre for Infection, Li Ka Shing Faculty of Medicine, The University of Hong Kong, Hong Kong, China

[3]Department of Infectious Disease and Microbiology, The University of Hong Kong-Shenzhen Hospital, Shenzhen, Guangdong, China

[4]Centre for Virology, Vaccinology and Therapeutics, Hong Kong Science and Technology Park, Hong Kong, China

[5]Academician Workstation of Hainan Province, Hainan Medical University—The University of Hong Kong Joint Laboratory of Tropical Infectious Diseases, Hainan Medical University, Haikou, Hainan, China

[6]The University of Hong Kong, Hong Kong, China

[7]Department of Microbiology, Queen Mary Hospital, Hong Kong, China

[8]Guangzhou Laboratory, Guangdong Province, China

[9]Department of Surgery, School of Clinical Medicine, Li Ka Shing Faculty of Medicine, The University of Hong Kong, Hong Kong, China

[10]CAS Key Laboratory of Quantitative Engineering Biology, Shenzhen Institute of Synthetic Biology, Shenzhen Institutes of Advanced Technology, Chinese Academy of Sciences, Shenzhen, Guangdong Province, China

Correspondence
Hin Chu, State Key Laboratory of Emerging Infectious Diseases, Department of Microbiology, School of Clinical Medicine, Carol Yu Centre for Infection, Li Ka Shing Faculty of Medicine, The University of Hong Kong, Hong Kong, China.
Email: hinchu@hku.hk

Abstract

Interferons (IFNs) are critical for immune defense against pathogens. While type-I and -III IFNs have been reported to inhibit SARS-CoV-2 replication, the antiviral effect and mechanism of type-II IFN against SARS-CoV-2 remain largely unknown. Here, we evaluate the antiviral activity of type-II IFN (IFNγ) using human lung epithelial cells (Calu3) and ex vivo human lung tissues. In this study, we found that IFNγ suppresses SARS-CoV-2 replication in both Calu3 cells and ex vivo human lung tissues. Moreover, IFNγ treatment does not significantly modulate the expression of SARS-CoV-2 entry-related factors and induces a similar level of pro-inflammatory response in human lung tissues when compared with IFNβ treatment.

Dong Yang, Jasper Fuk-Woo Chan, and Chaemin Yoon contributed equally to this study.

Mechanistically, we show that overexpression of indoleamine 2,3-dioxygenase 1 (IDO1), which is most profoundly induced by IFNγ, substantially restricts the replication of ancestral SARS-CoV-2 and the Alpha and Delta variants. Meanwhile, loss-of-function study reveals that IDO1 knockdown restores SARS-CoV-2 replication restricted by IFNγ in Calu3 cells. We further found that the treatment of L-tryptophan, a substrate of IDO1, partially rescues the IFNγ-mediated inhibitory effect on SARS-CoV-2 replication in both Calu3 cells and ex vivo human lung tissues. Collectively, these results suggest that type-II IFN potently inhibits SARS-CoV-2 replication through IDO1-mediated antiviral response.

KEYWORDS
COVID-19, ex vivo human lung tissues, IDO1, indoleamine 2,3-dioxygenase, interferon, SARS-CoV-2, type-II IFN

1 | INTRODUCTION

The coronavirus disease 2019 (COVID-19) pandemic caused by severe acute respiratory syndrome coronavirus 2 (SARS-CoV-2) resulted in over 772 million confirmed cases and more than 6 million deaths globally.[1] While the pandemic phase of SARS-CoV-2 is considered over, the latest variant of the concern of the virus, SARS-CoV-2 Omicron, has evolved to robustly escape the host adaptive immune response while gained a replication fitness in the upper respiratory tract.[2–7] These unique features of Omicron have allowed the virus to continuously circulate in the human population. Interferon (IFN) signaling plays critical roles in COVID-19 pathogenesis and interventions. While type-I and -III IFNs have been reported to inhibit SARS-CoV-2 replication in multiple models,[8–10] the antiviral role of type-II IFN in SARS-CoV-2 infection remains incompletely understood.

The host IFN system is part of the innate immune response, which plays an essential roles in the defense against pathogens.[11,12] In humans, IFNs are comprised of a diverse family of cytokines, including type-I (IFNα, IFNβ, IFNε, IFNκ, and IFNω), -II (IFNγ), and -III IFNs (IFNλ1, IFNλ2, and IFNλ3).[11] IFNs carry out potent antiviral activities through diverse mechanisms,[11,13,14] such as (i) the JAK-STAT (Janus activated kinase-signal transducer and activator of transcription); (ii) the mitogen-activated protein kinase (MAPK); and (iii) the PI3K/AKT/mTOR (phosphatidylinositol 3-kinase/serine-threonine kinase/mammalian target of rapamycin) signaling pathways. SARS-CoV-2 has been demonstrated to be highly sensitive to type-I and -III IFN in multiple models [8,9,15] and clinical benefits of type-I IFNs were reported in some clinical trials.[16,17] However, SARS-CoV-2 can antagonize type-I IFN signaling through blockade of STAT1 and STAT2 nuclear translocation and phosphorylation.[18,19] Meanwhile, accumulating evidence suggests that the timing of type-I IFN treatment is critical for restricting viral replication as late IFN treatment could lead to inflammation and lung injury.[15] A recent study suggested that type-II IFN (IFNγ) could inhibit SARS-CoV-2 replication in vitro.[20] However, the antiviral activity of IFNγ in the lung and the underlying mechanisms remain largely unexplored.

We previously reported that human lung epithelial cells (Calu3) and type-I/-II pneumocytes in ex vivo human lung tissues are targets of SARS-CoV-2.[21,22] Here, we evaluated the antiviral activity of IFNγ and the related mechanism in the context of SARS-CoV-2 infection using Calu3 cells and ex vivo human lung tissues. Our results demonstrate that IFNγ, similar to type-I IFN (IFNβ), potently inhibited SARS-CoV-2 replication in both Calu3 cells and ex vivo human lung tissues. Moreover, IFNγ treatment induced a similar level of pro-inflammatory cytokine response when compared to IFNβ in ex vivo human lung tissues. Mechanistically, we identified indoleamine 2,3-dioxygenase 1 (IDO1) as a significantly upregulated gene in IFNγ-treated Calu3 cells and ex vivo human lung tissues. We demonstrate that overexpression of IDO1 dramatically suppressed the replication of ancestral SARS-CoV-2, B.1.1.7 (Alpha), and B.1.617.2 (Delta). Importantly, the loss-of-function study illustrated that the depletion of IDO1 attenuated the IFNγ-mediated antiviral effect on SARS-CoV-2 replication. Furthermore, treatment of L-tryptophan, a substrate of IDO1, partly restored SARS-CoV-2 replication restricted by IFNγ in Calu3 cells and ex vivo human lung tissues. These results indicated a potent antiviral activity of type-II IFN on SARS-CoV-2 infection through the IDO1-mediated response in Calu3 cells and ex vivo human lung tissues. Together, our study provided insights into potential intervention strategies against viral infections based on IFNγ and IDO1-mediated pathways.

2 | MATERIALS AND METHODS

2.1 | Cells and viruses

All cell lines were obtained from the American Type Culture Collection (ATCC).[23] VeroE6 and BHK21 cells were cultured in Dulbecco's Modified Eagle's Medium (DMEM) and Calu3 cells were cultured in DMEM/F12, respectively, supplemented with 10% fetal bovine serum (FBS), 100 units/mL penicillin and 100 μg/mL streptomycin. Ancestral SARS-CoV-2 (GeneBank accession number: MT230904), SARS-CoV-2 B.1.1.7 (GISAID: EPI_ISL_1273444) and B.1.617.2 (GISAID: EPI_ISL_3221329) were isolated from laboratory-confirmed COVID-19 patients and were cultured and titered in VeroE6-TMPRSS2 cells.[24] SARS-CoV-1 GZ50 (GenBank accession number: AY304495) was an archived clinical isolate at the Department of Microbiology, The University of Hong Kong. All experiments involving live SARS-CoV-2 or SARS-CoV-1 followed the approved standard operating procedures of the Biosafety Level 3 facility at Department of Hong Kong, The University of Hong Kong.[5,25]

2.2 | Ex vivo human lung tissue culture

All donors gave written consent as approved by the Institutional Review Board of the University of Hong Kong/Hospital Authority Hong Kong West Cluster. Human lung tissues obtained from patients undergoing surgical operations were processed into small rectangular pieces and were cultured with basal medium (Advanced DMEM/F12 supplemented with 2 mM of 4-(2-hydroxyethyl)−1-piperazineethanesulfonic acid (HEPES) (Gibco), 1×GlutaMAX (Gibco), 100 U/mL penicillin, and 100 μg/mL streptomycin) as we described previously.[21,26,27]

2.3 | RNA extraction and reverse transcription-quantitative real-time polymerase chain reaction (RT-qPCR)

RNA extraction and RT-qPCR analysis were performed as previously described.[19] In brief, RT-qPCR was used to quantify SARS-CoV-2 and SARS-CoV-1 genome copy numbers using QuantiNova Probe One-step RT-PCR kit (Qiagen) with Light-Cycler 96 Real-Time PCR System (Roche). The primer and probe sequences were designed to target viral RNA-dependent RNA polymerase/Helicase (RdRp/Hel) regions, and RNA extraction, reverse transcription, and quantitative PCR were performed as we described previously.[28] For host factors analysis, the IFN-treated ex vivo lung tissues were lysed using RLT buffer and the total RNA was extracted using RNA extraction kit, according to the manufacturer's instructions. The levels of cellular gene expression were normalized to GAPDH and presented as fold change in gene expression of treated cells relative to that of nontreated cells. Host genes analyzed included ACE2, FURIN, TMPRSS2, TNF-α, IL1β, IL6, IL8, IL12, IP10, IFIT1, IFIT2, IFIT3, IFITM3, ISG15, OAS1, TRIM22, PLSLR1, IDO1, and PKR. All primer sequences are provided in Table S1.

2.4 | Treatment of human lung epithelial cells and ex vivo human lung tissues with IFNs and SARS-CoV-2 infection

Human lung epithelial cells (Calu3) were mock-pretreated or pretreated with human recombinant IFNβ, IFNγ, or IFNλ1 at the indicated concentrations for 16 h. We treated Calu3 and ex vivo lung tissues with IFNλ at the concentration from 100 to 1000 ng/mL.[20,29] The cells were then infected with SARS-CoV-2 at a multiplicity of infection (MOI) of 2. After 2 h of incubation, the virus inoculum was washed off and the cells were maintained in DMEM/F12 containing IFNβ, IFNγ, or IFNλ1. The cell lysates and supernatants were harvested for RT-qPCR detection at 24 h postinfection (hpi). For ex vivo human lung tissues, the processed tissues were mock-pretreated or pretreated with human recombinant IFNβ, IFNγ, IFNλ1, or a combination of IFNλ (IFNλ1, IFNλ2, and IFNλ3) at the indicated concentrations for 16 h. The tissues were subsequently infected with 1×10^7 PFU/mL of SARS-CoV-2 with the same concentration of corresponding human recombinant IFNs for 2 h and washed with phosphate-buffered saline (PBS) three times. The infected tissues were

maintained with basal medium supplemented with 20 μg/mL vancomycin, 20 μg/mL ciprofloxacin, 50 μg/mL amikacin, 50 μg/mL nystatin, and indicated IFNs. After 24 h of inoculation, the tissues and supernatants were harvested for RT-qPCR and plaque assays, respectively.

2.5 | IFN treatment for evaluation of host gene expression in ex vivo human lung tissues

The processed ex vivo human lung tissues were treated with 2000 U/mL IFNβ, 2000 U/mL IFNγ, or 100 ng/mL IFNλ1. The tissue lysates were harvested at 16 h posttreatment for entry-related factors detection and at 24 h posttreatment for pro-inflammatory cytokines and ISGs detection. The tissue lysates were harvested for detection of host cellular genes by RT-qPCR and normalized with GAPDH. The gene expression fold change was normalized to that of the mock-treated controls.

2.6 | IDO1 expression in IFNγ-treated Calu3 cells and ex vivo human lung tissues

Calu3 cells and ex vivo human lung tissues were mock-treated or treated with recombinant IFNγ at the indicated concentration (75, 125, 250, 500, 1000, and 2000 U/mL). After 24 h, the cell lysates and the tissue lysates were collected for evaluation of IDO1 expression by RT-qPCR normalized with GAPDH. Data were presented as fold change relative to mock treatment.

2.7 | Overexpression and virus infection

BHK21 cells were transfected with 1 μg of control vector, 1 μg of plasmid expressing human ACE2 (hACE2) (Sino Biological), or cotransfected with 1 μg of plasmid expressing hACE2 and 1 μg of plasmid expressing IDO1 (Sino Biological) using Lipofectamine 3000 (Thermo Fisher Scientific). After 24 h, the transfected cells were infected with SARS-CoV-1, SARS-CoV-2, or variants of SARS-CoV-2 at an MOI of 0.2. The cell lysates and supernatants were collected to determine the viral genome and live infectious virus by RT-qPCR and plaque assays at 24 and 48 hpi. The viral gene expressions were normalized to mouse β-actin and fold change was calculated to vector-transfected controls in cell lysate samples.

2.8 | siRNA knockdown and IFNγ treatment

Calu3 cells were transfected with 70 nM siRNA targeting IDO1 obtained from Dharmacon using RNAiMAX (Thermo Fisher Scientific) for three consecutive days, with scrambled siRNA as negative controls, followed by nontreatment or treatment with

IFNγ (2000 U/mL) for another 24 h. After 24 h treatment, the cells were infected with SARS-CoV-2 at an MOI of 1. The cell lysates and supernatants were harvested at 24 hpi for detection of viral genome copy and live infectious virus by RT-qPCR and plaque assays, respectively.

2.9 | Western blots

Western blots were performed as we previously described with slight modifications.[30] After 24 h transfection, the transfected BHK21 cells with control vector and the cells cotransfected with ACE2 and IDO1 were lysed with RIPA buffer (Thermo Fisher Scientific) supplemented with a protease inhibitor cocktail (Thermo Fisher Scientific). The expression levels of hACE2, IDO1, and β-actin were detected by Western blot using rabbit anti-V5 (R&D), mouse anti-Flag (Sigma-Aldrich), and mouse anti-β-actin (Sigma-Aldrich) primary antibodies, respectively.

2.10 | Quantitative analysis of L-Trp by liquid chromatography–tandem mass spectrometry (LC–MS/MS)

Calu3 cells were transfected with control siRNA and siRNA targeting IDO1 for 3 consecutive days. Similarly, Calu3 cells were untreated or treated with 2000 U/mL IFNγ for 24 h. The cells were washed with PBS and then treated with 80% (vol/vol) methanol with L-Trp-d5 as an internal control. The cells were harvested with a cell scraper followed by vacuum drying. LC-MS/MS was applied on the harvested samples to evaluate L-Trp with QTRAP 6500 LC-MS/MS System.

2.11 | L-Tryptophan (L-Trp) rescue assay

Calu3 cells and ex vivo human lung tissues were mock-pretreated or pretreated with IFNγ (2000 U/mL) accompanied without or with L-Trp at the indicated concentrations for 24 h. The treated cells or human lung tissues were infected with SARS-CoV-2 at 0.1 MOI or viral stock (1×10^7 PFU/mL) at 37°C, respectively. After 2 h of incubation, the cells and the human lung tissues were washed with PBS and incubated medium containing IFNγ (2000 U/mL) and the different concentrations of L-Trp. The cell lysates and supernatants were harvested at 48 hpi to determine viral genome copy by RT-qPCR.

2.12 | Statistical analysis

The data are presented as means and standard deviations. Student's *t* test, one-way ANOVA, and two-way ANOVA were used for statistical analysis. Differences were considered significant when $p < 0.05$. $^*p < 0.05$, $^{**}p < 0.01$, $^{***}p < 0.001$, and $^{****}p < 0.0001$.

3 | RESULTS

3.1 | Type-II IFN inhibits SARS-CoV-2 replication in human lung epithelial cells and ex vivo human lung tissues

The human respiratory tract is the primary target of SARS-CoV-2.[31] The human lung epithelial cells, Calu3, are highly susceptible to SARS-CoV-2 infection.[22,23] Here, we first examined the antiviral activities of type-II IFN (IFNγ) against SARS-CoV-2 in Calu3 cells. Type-I (IFNβ) and -III IFN (IFNλ1) that are known to restrict SARS-CoV-2 replication were included as control groups for comparison.[8,9,16] Calu3 cells were pretreated with IFNγ, IFNβ, and IFNλ1 at the indicated concentrations for 16 h. The pretreated Calu3 cells were then infected with SARS-CoV-2 ancestral strain and cultured with fresh medium supplemented with different IFNs accordingly. The supernatants and cell lysates were collected at 24 hpi for determining viral genome copy by RT-qPCR (Figure 1A). Our results demonstrated that both IFNβ and IFNλ1 inhibited SARS-CoV-2 replication in a dose-dependent manner in the cell lysate and supernatant samples of Calu3 cells. Importantly, SARS-CoV-2 replication was also significantly suppressed in IFNγ-treated Calu3 cells (Figure 1B,C). Even at the lowest evaluated concentration (125 U/mL), IFNγ treatment reduced SARS-CoV-2 replication to 39.50% ($p < 0.0001$) and 44.44% ($p = 0.0003$) of that of the mock treatment in the cell lysates and supernatants, respectively (Figure 1B,C).

To resemble a more physiologically relevant condition, we evaluated the antiviral effect of IFNγ on SARS-CoV-2 infection using ex vivo human lung tissues. As shown in Figure 2A, we infected fresh ex vivo human lung tissues from three donors with SARS-CoV-2, followed by treatment with IFNβ (2000 U/mL), IFNγ (2000 U/mL), or IFNλ1 (100 ng/mL).[9,29] After 24 h of incubation, the tissue lysates were harvested to determine viral RdRp genome copy by RT-qPCR and the supernatants were collected for detection of live infectious virus by plaque assays. Similar to the results from Calu3 cells, all IFNs inhibited SARS-CoV-2 replication in ex vivo human tissues (Figure 2B). Next, we further assessed the antiviral activity of IFNγ on SARS-CoV-2 replication with pretreatment and posttreatment in ex vivo human lung tissues as shown in Figure 2C. In this setting, treatment of IFNγ inhibited SARS-CoV-2 infectious titer in ex vivo human lung tissues by 17.57-fold (Donor D, $p = 0.0002$), 13.70-fold
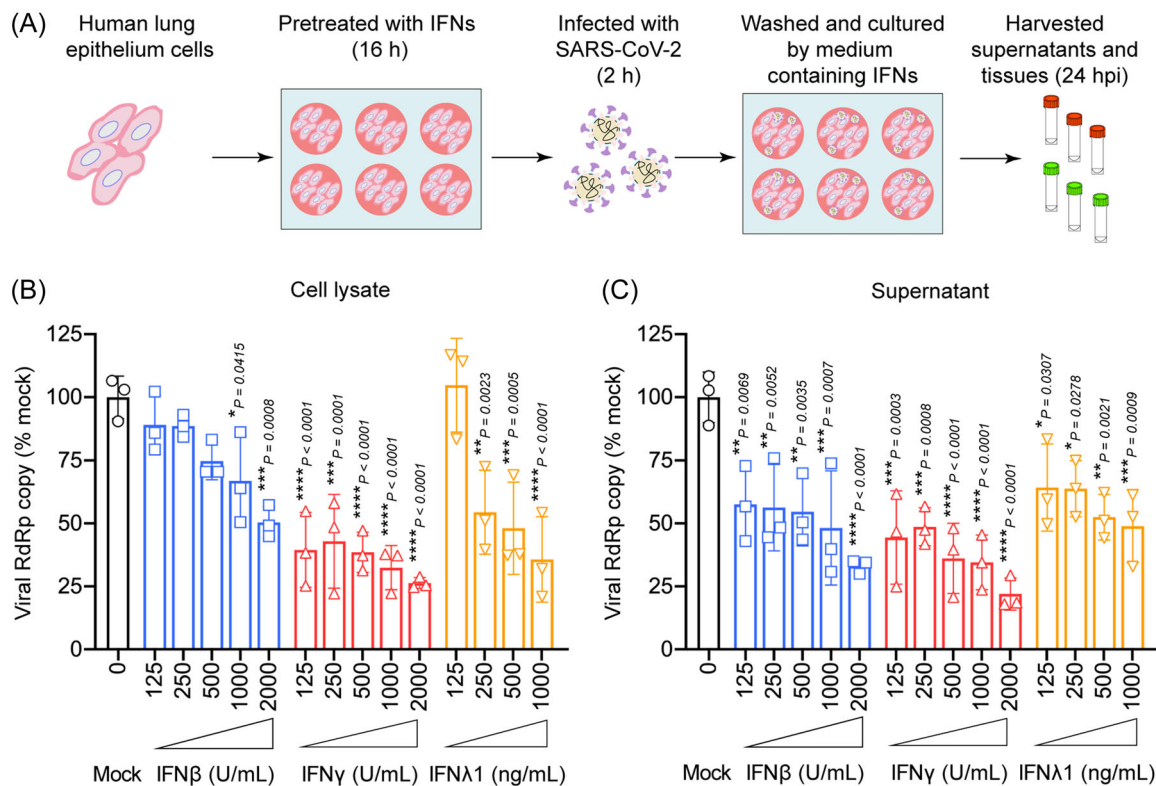

FIGURE 1 Type-II IFN inhibits SARS-CoV-2 replication in human lung epithelial cells. (A) Schematic illustration of the IFNs treatment and SARS-CoV-2 infection in human lung epithelial cells (Calu3). (B) Antiviral activity of IFNs against SARS-CoV-2 in Calu3 cells. Calu3 cells were mock-treated or pretreated with distinct IFNs (IFNβ, IFNγ, and IFNλ1) at the indicated concentrations for 16 h and infected with SARS-CoV-2 at an MOI of 2 for 2 h. The infected cells were washed and incubated with fresh medium supplemented with or without corresponding IFNs. After 24 h postinfection, the viral genome copy in cell lysates and supernatants was determined by RT-qPCR. Viral gene expression was normalized to mock-treated controls. $n = 3$. Data are mean ± s.d. from the indicated number of biological repeats. Statistical analyses in all panels were performed with one-way ANOVA (Dunnett's multiple comparisons test) and the differences were considered significant when $p < 0.05$. *$p < 0.05$, **$p < 0.01$, ***$p < 0.001$, and ****$p < 0.0001$.
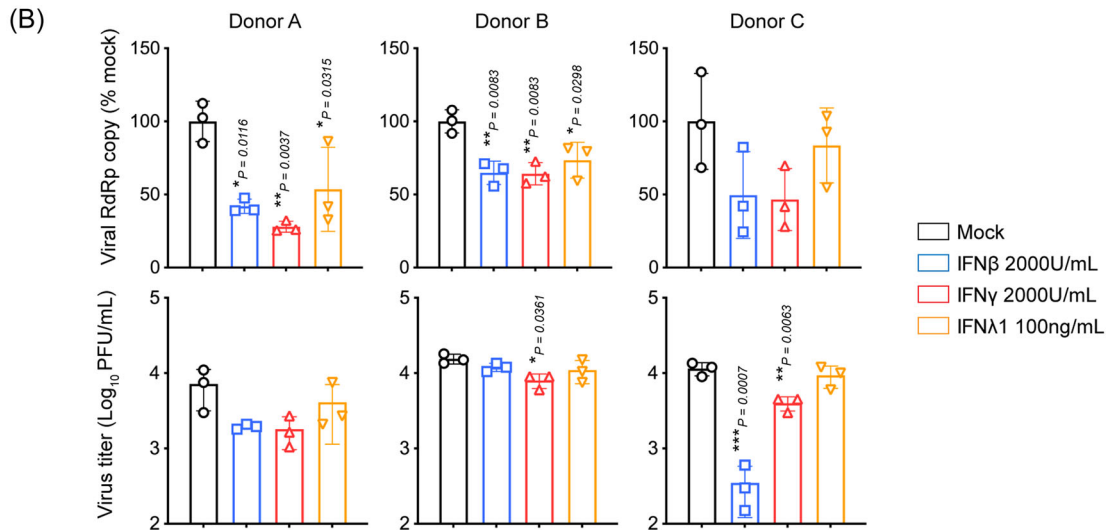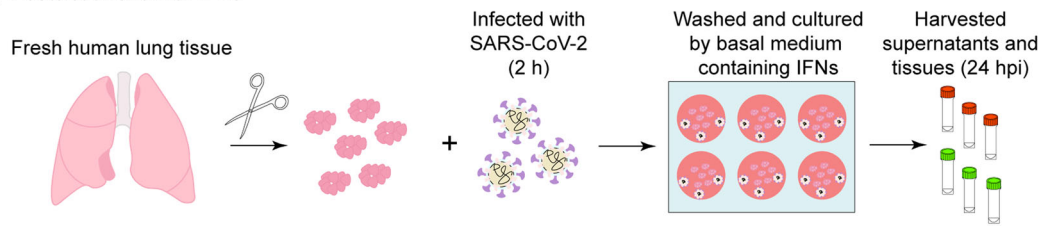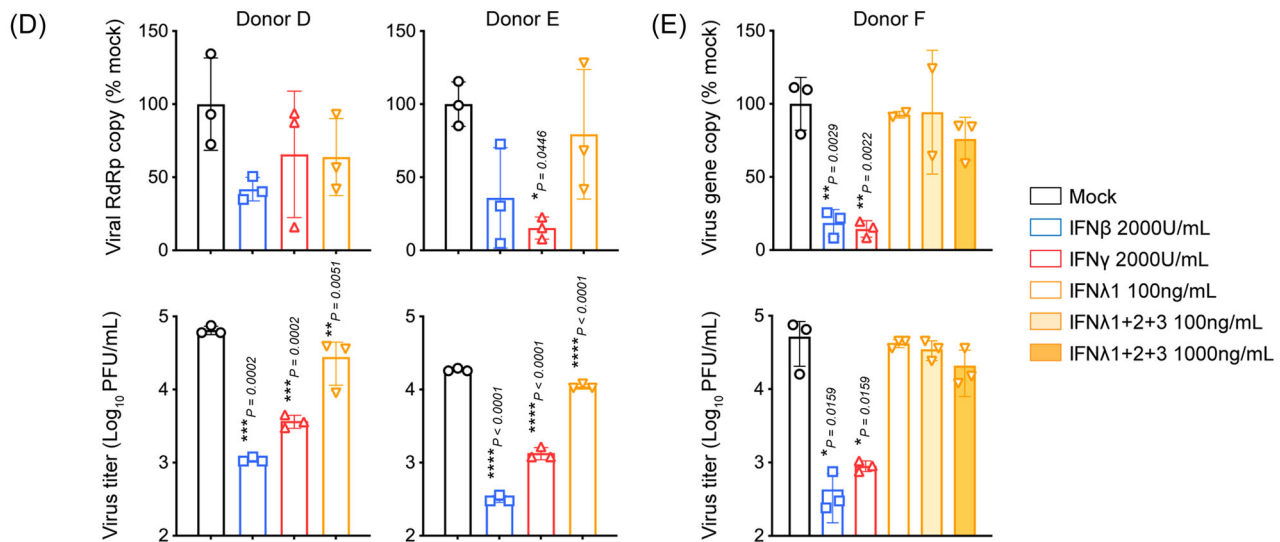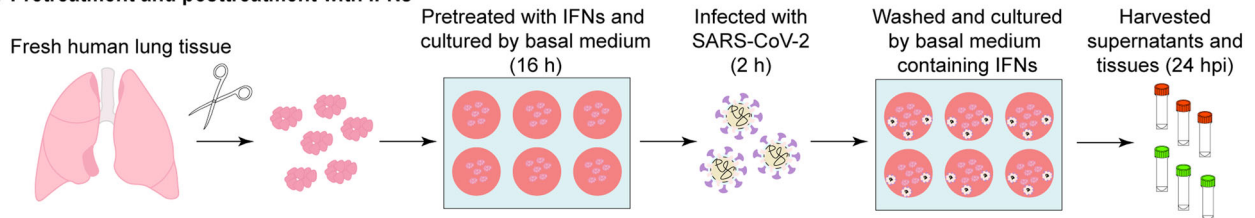
FIGURE 2 (See caption on next page).

(Donor E, $p < 0.0001$), or 57.78-fold (Donor F, $p = 0.0159$) when compared to mock-treated samples, respectively (Figure 2D,E, lower panels). Likewise, IFNγ treatment dramatically reduced viral genome copy in the tissue samples by 34.31% (Donor D, $p = $ ns), 84.74% (Donor E, $p = 0.0446$), and 85.52% (Donor F, $p = 0.0022$) in comparison with mock-treated samples, respectively (Figure 2D,E, upper panels). Interestingly, we detected limited anti-SARS-CoV-2 effect by IFNλ1 in the ex vivo human lung tissues at the evaluated concentrations (Figure 2D,E), even when with a combination of 1000 ng/mL IFNλ1, 1000 ng/mL IFNλ2, and 1000 ng/mL IFNλ3 were applied (Figure 2E). Collectively, these findings demonstrate that type-II IFN efficiently suppresses SARS-CoV-2 replication in ex vivo human lung tissues.

3.2 | Type-II IFN does not significantly alter the expression of SARS-CoV-2 entry-related factors in ex vivo human lung tissues

Recent studies reported that SARS-CoV-2 receptor angiotensin-converting enzyme 2 (ACE2) can be upregulated by IFN treatment in vitro.[20,32] Here, we evaluated the expression level of the known SARS-CoV-2 entry-related factors in IFNγ-treated ex vivo human lung tissues, including ACE2, transmembrane protease serine 2 (TMPRSS2), and FURIN. As shown in Figure 3A, fresh ex vivo lung tissues from three donors were treated with individual IFNs and were collected for detection of gene expression by RT-qPCR at 16 h posttreatment. Our results showed that IFNβ, but not IFNγ and IFNλ1, significantly upregulated a novel truncated isoform of ACE2 (delta ACE2, dACE2) expression, while all types of IFN did not significantly upregulate total ACE2 expression (full-length ACE2 and dACE2) due to the lower expression level of endogenous dACE2 in ex vivo human lung tissues (Figures 3B, S1, and S2). These observations are consistent with previous findings that interferons, specifically type-I IFNs (IFNα and IFNβ) can induce the expression of dACE2, but not full-length ACE2.[33] Collectively, our results demonstrate that the

evaluated IFNs do not significantly alter the expression of ACE2, FURIN, and TMPRSS2 in ex vivo human lung tissues (Figure 3B).

3.3 | Type-II IFN does not significantly upregulate pro-inflammatory cytokines/chemokines production in ex vivo human lung tissues, except IP10

Given the adverse role of the exaggerated pro-inflammatory response in COVID-19 patients, we examined whether IFNγ treatment would initiate pro-inflammatory cytokines/chemokines production in ex vivo human lung tissues. The human lung tissues were treated with IFNγ for 24 h, and the mRNA level of representative cytokines were examined by RT-qPCR. IFNβ and IFNλ1 were included as control treatments. We found that IFNβ and IFNγ did not significantly increase the expression level of TNF-α, IL1β, IL6, and IL8 in the treated ex vivo human lung tissues (Figures 4 and S3). Of note, IFNβ and IFNγ, but not IFNλ1, significantly upregulated IP10 expression to comparable levels (Figure 4). Importantly, we found that all types of IFN did not significantly induce cell death in Calu3 cells, suggesting an antiviral activity without substantial cellular cytotoxicity of IFNγ (Figure S4). These results demonstrate that type-II IFN does not trigger profound pro-inflammatory responses in ex vivo human lung tissues.

3.4 | Type-II IFN triggers a potent antiviral state in ex vivo human lung tissues

To assess antiviral response upon IFNγ treatment in ex vivo human lung tissues, we quantified the mRNA expression level of a set of representative interferon-stimulated genes (ISGs) that have been implicated to mediate antiviral effects.[34,35] The ex vivo lung tissues were treated with IFNs for 24 h and were harvested to analyze the production of ISGs by RT-qPCR, including interferon-induced protein with tetratricopeptide repeats 1 (IFIT1), IFIT2,

---

FIGURE 2 Type-II IFN inhibits SARS-CoV-2 replication in ex vivo human lung tissues. (A) Schematic diagram of the IFNs posttreatment and SARS-CoV-2 infection in ex vivo human lung tissues. (B) Antiviral activity of IFNs against SARS-CoV-2 in ex vivo human lung tissues. The fresh human lung samples from three donors were cut into small rectangular pieces and infected with SARS-CoV-2 viral stock (Viral titer: 10^7 PFU/mL, determined by plaque assays in VeroE6 cells). The infected ex vivo human lung tissues were washed with PBS and then cultured with basal medium supplemented without or with 2000 U/mL IFNβ, 2000 U/mL IFNγ, and 100 ng/mL IFNλ1, respectively. After 24 h incubation, the tissue lysates and supernatants were harvested for detection of viral genome copy and live infectious virus by RT-qPCR and plaque assays, respectively. Viral gene expression was normalized to mock-treated controls. $n = 3$. (C) Schematic diagram of pretreatment and posttreatment of IFNs and SARS-CoV-2 infection in ex vivo human lung tissues. (D and E) Antiviral activity of IFNs against SARS-CoV-2 in ex vivo human lung tissues. The fresh human lung samples from three donors were cut into small rectangular pieces and then mock-treated or pretreated with 2000 U/mL IFNβ, 2000 U/mL IFNγ, 100 ng/mL IFNλ1, 100 ng/mL IFNλs (IFNλ1+λ2+λ3), or 1000 ng/mL IFNλs for 16 h, respectively. The treated ex vivo human lung tissues were infected with SARS-CoV-2 viral stock for 2 h. The infected ex vivo human lung tissues were washed with PBS and cultured with basal medium supplemented without or with corresponding IFNs at the same concentration as pretreatment, respectively. After 24 h incubation, the tissue lysates and supernatants were harvested for detection of viral genome copy and live infectious viral particle by RT-qPCR and plaque assays, respectively. Viral gene expression was normalized to mock-treated controls. $n = 3$. Data are mean ± s.d. from the indicated number of biological repeats. Statistical analyses in all panels were performed with one-way ANOVA (Holm-Sidak's multiple comparisons test) and the differences were considered significant when $p < 0.05$. *$p < 0.05$, **$p < 0.01$, ***$p < 0.001$, and ****$p < 0.0001$.
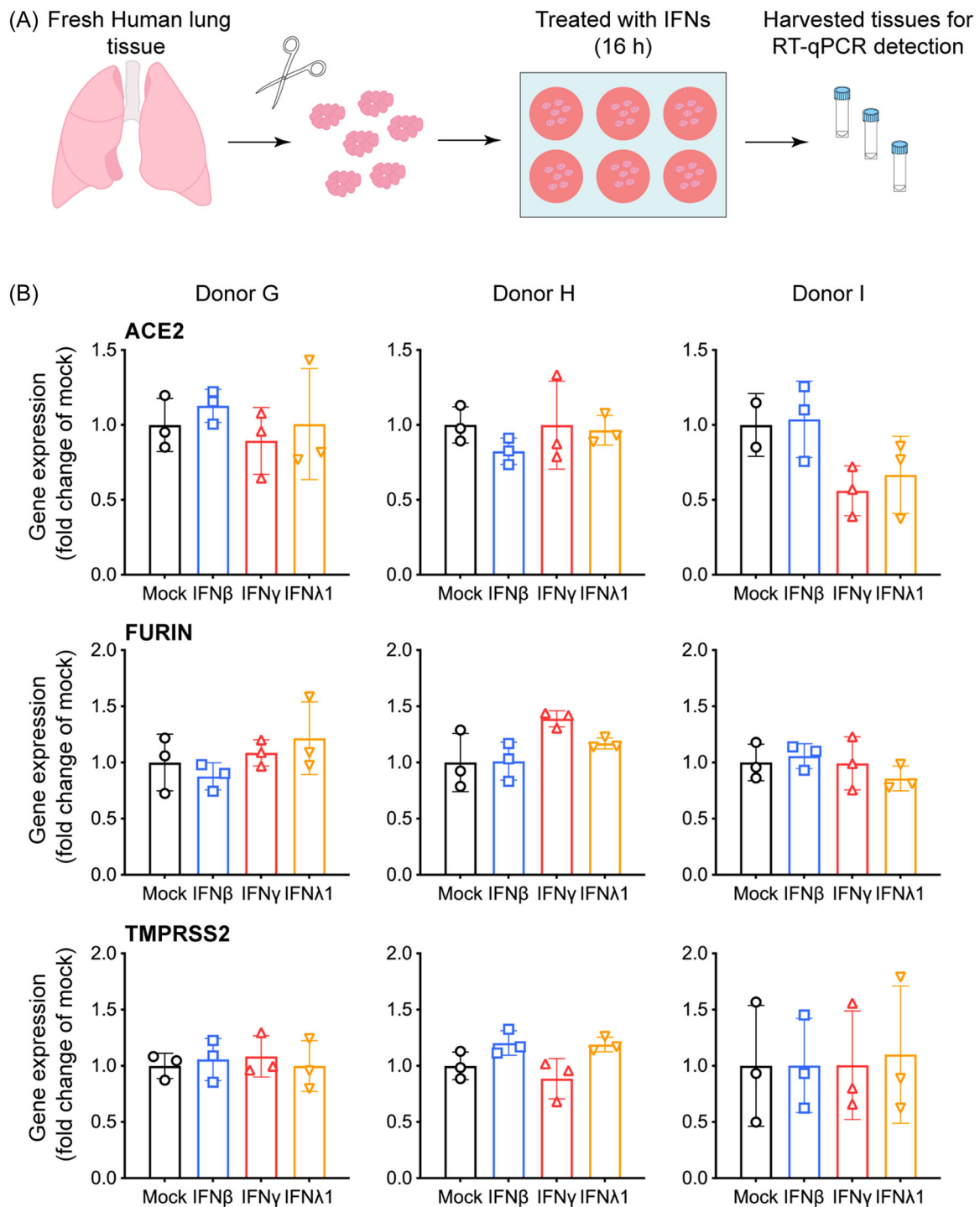
FIGURE 3 Type-II IFN treatment does not affect the expression of SARS-CoV-2 entry-related factors in ex vivo human lung tissues. (A) Schematic illustration of the IFNs treatment in ex vivo human lung tissues. (B) The expression levels of SARS-CoV-2 entry-related factors in IFN-treated ex vivo human lung tissues. The procedure of generation of ex vivo human lung tissues was the same as Figure 2 described. The ex vivo human lung tissues were treated with 2000 U/mL IFNβ, 2000 U/mL IFNγ, and 100 ng/mL IFNλ1, respectively. After 16 h, the tissue lysates were harvested for detection of viral entry-related factors by RT-qPCR and normalized to GAPDH. Data are presented as fold change relative to mock-treated controls. $n = 3$. Data are mean ± s.d. from the indicated number of biological repeats. Statistical analyses in all panels were performed with one-way ANOVA (Holm-Sidak's multiple comparisons test) and the differences were considered significant when $p < 0.05$.

IFIT3, ISG15, 2′-5′-oligoadenylate synthetase 1 (OAS1), interferon-induced transmembrane protein 3 (IFITM3), tripartite motif-containing 22 (TRIM22), phospholipid scramblase 1 (PLSCR1), indole 2,3-dioxygenase 1 (IDO1), and protein kinase K (PKR). Our results showed that a majority of the ISGs examined were upregulated in all IFN-treated ex vivo human lung tissues as compared to that in mock-treated tissues (Figures 5A and S5). Intriguingly, among all examined ISGs, IFNγ most remarkably

FIGURE 4 Type-II IFN does not affect pro-inflammatory response in ex vivo human lung tissues, except IP10. The ex vivo human lung tissues were treated with 2000 U/mL IFNβ, 2000 U/mL IFNγ, and 100 ng/mL IFNλ1, respectively. The tissue lysates were harvested at 24 h posttreatment for detection of cytokines/chemokines by RT-qPCR and normalized to GAPDH. Data are presented as fold change relative to mock-treated controls. $n = 3$. Data are mean ± s.d. from the indicated number of biological repeats. Statistical analyses in all panels were performed with one-way ANOVA (Holm-Sidak's multiple comparisons test) and the differences were considered significant when $p < 0.05$. $*p < 0.05$, $**p < 0.01$, $***p < 0.001$, and $****p < 0.0001$.
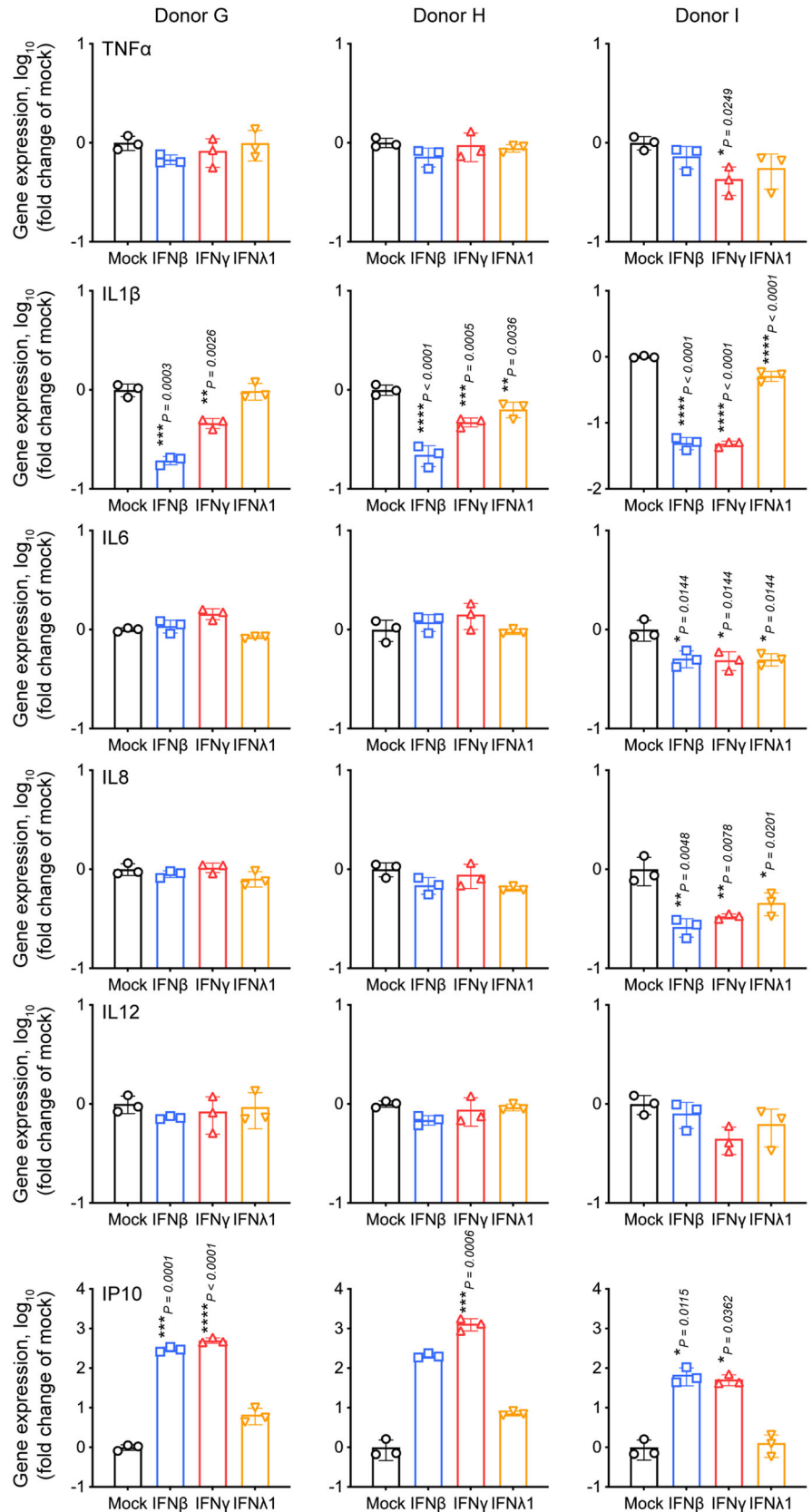
induced IDO1 expression as demonstrated by the 133.08- (Donor G, $p < 0.0001$), 94.81- (Donor H, $p = 0.0142$), and 27.85- (Donor I, $p = 0.0013$) fold increase in ex vivo human lung tissues (Figure 5A), which is in line with previous studies suggesting that IFNγ is a potent cytokine to stimulate IDO1 expression.[36] Our findings illustrate that type-II IFN treatment can activate a potent antiviral response with an exceptional expression of IDO1 in ex vivo human lung tissues.
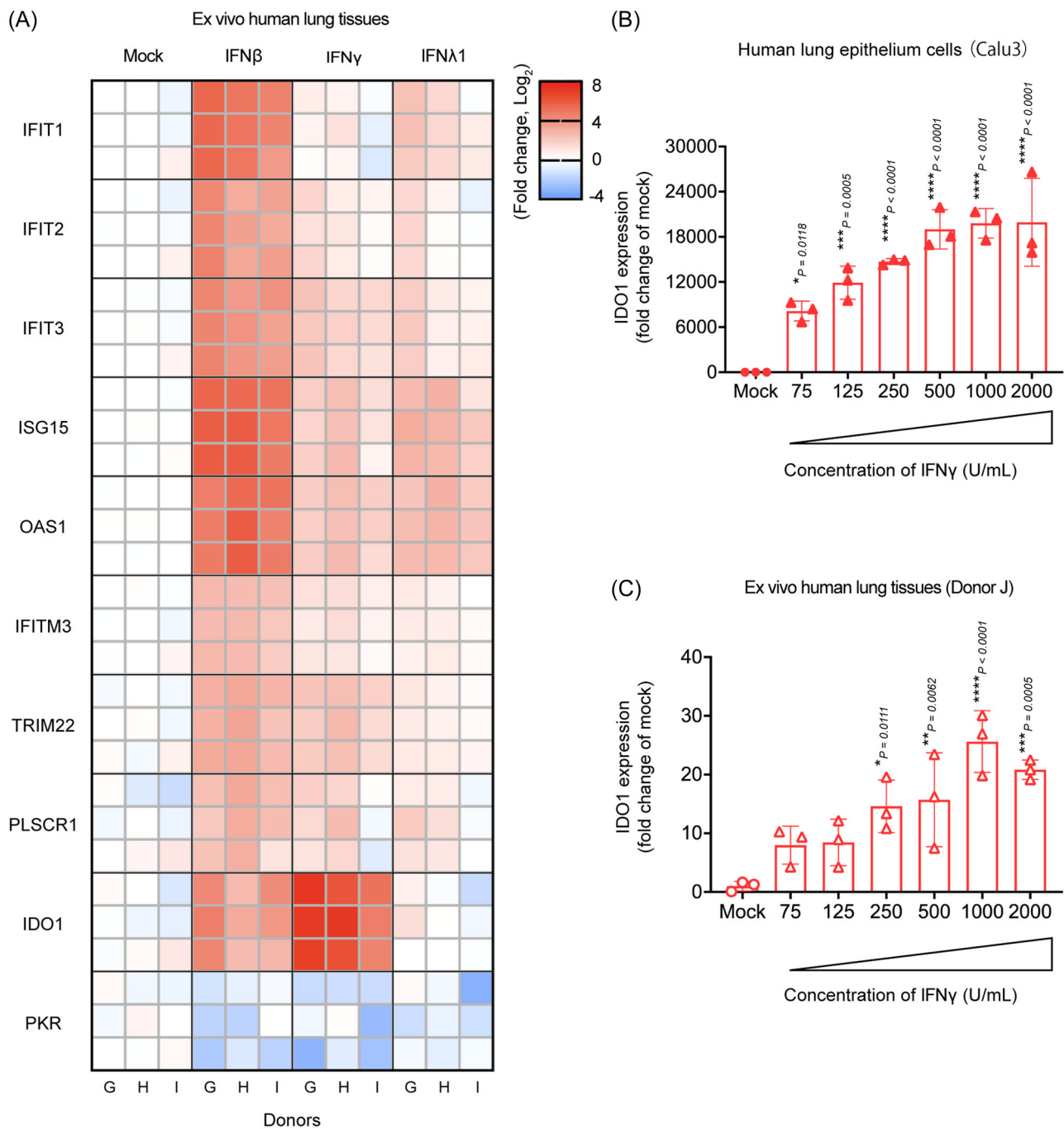
FIGURE 5 Type-II IFN induces an antiviral response in ex vivo human lung tissues. (A) The heatmap of representative interferon-stimulated genes (ISGs) expression in IFN-treated ex vivo human lung tissues. The methods were the same as Figure 4 described. The tissue lysates were harvested for the detection of ISGs by RT-qPCR and normalized to GAPDH. Data are presented as fold change relative to mock treatment. n = 3. (B) IDO1 expression in IFNγ treated Calu3 cells. Calu3 cells were treated with IFNγ at the indicated concentrations for 24 h. The cell lysates were harvested for the detection of IDO1 by RT-qPCR and normalized to GAPDH. Data are presented as fold change relative to mock treatment. n = 3. (C) IDO1 expression in IFNγ treated ex vivo human lung tissues. The procedure of generation of ex vivo human lung tissues was the same as Figure 2 described. The methods of the IFNγ treatment were the same as (B) described. n = 3. Data are mean ± s.d. from the indicated number of biological repeats. Statistical analyses in all panels were performed with one-way ANOVA (Dunnett's multiple comparisons test) and the differences were considered significant when $p < 0.05$. *$p < 0.05$, **$p < 0.01$, ***$p < 0.001$, and ****$p < 0.0001$.
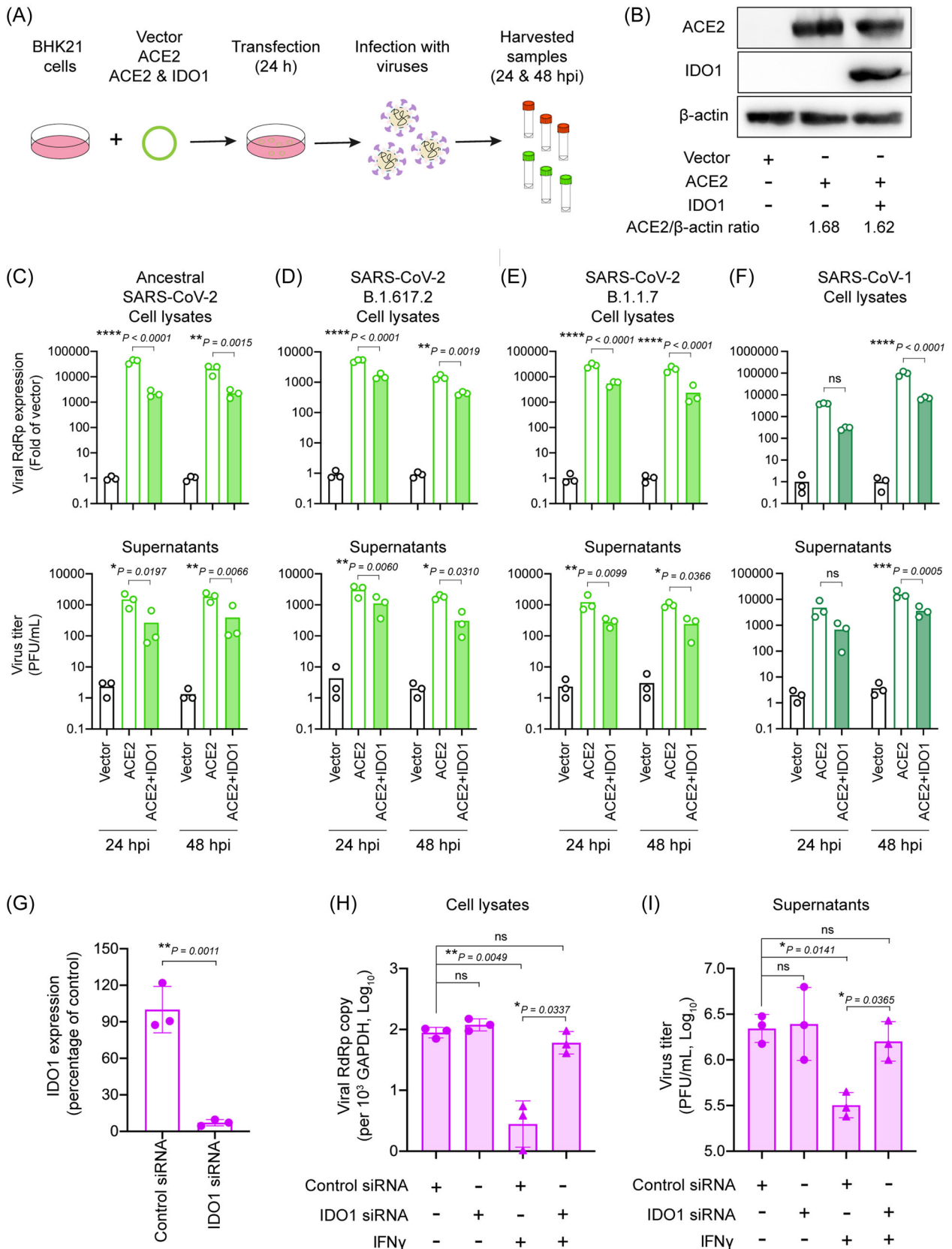
FIGURE 6 (See caption on next page).

3.5 | Type-II IFN upregulates IDO1 expression in human lung epithelial cells and ex vivo human lung tissues

Next, we treated Calu3 cells and ex vivo human lung tissues with different concentrations of IFNγ and quantified the expression of IDO1 using RT-qPCR. Our data revealed that 2000 U/mL IFNγ robustly stimulated IDO1 expression by 19941 folds ($p < 0.0001$) in comparison with that of mock-treated Calu3 cells (Figure 5B). IDO1 induction by IFNγ is highly robust since we detected an 8144-fold induction of IDO1 in IFNγ-treated cells even at a concentration as low as 75 U/mL ($p = 0.0118$). Similarly, although the magnitude of IDO1 upregulation in IFNγ-treated ex vivo human lung tissues was lower than that in Calu3 cells, IFNγ induced IDO1 production by 8.0–20.8 folds in ex vivo human lung tissues in a dose-dependent manner (Figure 5C). These results indicate that IDO1 expression can be specifically and potently upregulated by IFNγ in Calu3 cells and ex vivo human lung tissues.

3.6 | Type-II IFN inhibits SARS-CoV-2 replication in an IDO1-dependent manner

A recent study reported that tryptophan (Trp) metabolism and kynurenine (Kyn) pathway were substantially activated in COVID-19 patients.[37] IDO1, which is also elevated in COVID-19 patients, catalyzes the rate-limiting step of Trp degradation along the Kyn pathway.[38,39] We similarly found that SARS-CoV-2 can induce IDO1 upregulation in ex vivo human lung tissues (Figure S6). IDO1-mediated antiviral effects have been recognized for other pathogens such as hepatitis B virus (HBV), herpes simplex virus type 2 (HSV-2), and human immunodeficiency virus 1(HIV-1).[36,40,41] Therefore, we further explored whether the IDO1-mediated pathway could modulate SARS-CoV-2 replication. The BHK21 cell line is commonly used as a mammalian cell transient transfection model isolated from the kidney of golden hamster. We transfected BHK21 cells with human

ACE2 (hACE2) and IDO1 or hACE2 alone followed by infection with SARS-CoV-1, ancestral SARS-CoV-2, SARS-CoV-2 Delta (B.1.617.2), or SARS-CoV-2 Alpha (B.1.1.7). The supernatants and cell lysates were collected for virus detection at 24 and 48 hpi as shown in Figure 6A. Western blots assay revealed that hACE2 was successfully expressed in BHK21 cells. In addition, both hACE2 and IDO1 expression can be detected in cotransfected cells, and cotransfection of IDO1 did not reduce hACE2 expression (Figure 6B). We found that hACE2 transfection dramatically promoted replication of all evaluated viruses in BHK21 cells compared to transfection with empty vector in both cell lysate and supernatant samples (Figure 6C–F). Importantly, cotransfection of IDO1 with hACE2 significantly reduced ancestral SARS-CoV-2 replication by 18.68-fold ($p < 0.0001$) and 9.06-fold ($p = 0.0015$) in cell lysates at 24 and 48 hpi in comparison with hACE2 transfection alone (Figure 6C). Importantly, our data also demonstrated that overexpression of IDO1 reduced the replication of SARS-CoV-2 Alpha and Delta variants in hACE2-transfected BHK21 cells, as evidenced by 2.70–5.80 folds and 3.27–8.50 folds decrease in the supernatants and cell lysates, respectively (Figure 6D,E). In addition to SARS-CoV-2, SARS-CoV-1 replication was similarly restricted by IDO1 when compared to cells transfected with hACE2 alone (Figure 6F).

Next, we performed loss-of-function studies to further investigate the role of IDO1 on SARS-CoV-2 replication. As illustrated in Figure 6G, transfection of siRNA targeting IDO1 significantly diminished the expression of IDO1 by 92.85% ($p = 0.0011$) compared to control siRNA transfection in Calu3 cells. Furthermore, Calu3 cells were treated with IFNγ after siRNA transfection, followed by infection of SARS-CoV-2. The results showed a marginal increase in viral genome copy number and virus titer after IDO1 knockdown, which was not statistically significant. In keeping with our earlier observation, IFNγ treatment significantly inhibited SARS-CoV-2 replication in Calu3 cells. Strikingly, the addition of IDO1 depletion robustly rescued SARS-CoV-2 replication that was inhibited by IFNγ treatment ($p = 0.0337$) in cell lysate samples (Figures 6H and S7). Similarly, IDO1 depletion also significantly rescued SARS-CoV-2

FIGURE 6 Type-II IFN inhibits SARS-CoV-2 replication in an IDO1-mediated response. (A) Schematic diagram of the transfection of plasmids and virus infection. (B) Detection of human ACE2 and IDO1 in transfected BHK21 cells by Western blots. BHK21 cells were transfected with 1 μg of control vector or cotransfected with 1 μg of a plasmid expressing human ACE2 and 1 μg of a plasmid expressing IDO1. After 24 h, the cell lysates were lysed with RIPA buffer and collected for the detection of ACE2, IDO1, and β-actin by Western blots. (C–F) Overexpression of IDO1 in BHK21 cell inhibits replications of (C) the ancestral SARS-CoV-2 and the variants including (D) B.1.617.2 and (E) B.1.1.7, (F) SARS-CoV-1. After 24 h transfection, the transfected cells were infected with distinct viruses at an MOI of 0.2. The supernatants and cell lysates were harvested at 24 and 48 hpi for detection of live infectious virus and viral genome copy by plaque assays and RT-qPCR, respectively. $n = 3$. (G) knockdown efficiency of siRNA transfection was determined by RT-qPCR. Calu3 cells were transfected with control siRNA and siRNA targeting IDO1 for 3 consecutive days. The cell lysates were harvested for detection of mRNA level of IDO1. Data are presented as percentage relative to control siRNA. $n = 3$. (H and I) The depletion of IDO1 rescues SARS-CoV-2 replication upon IFNγ treatment. After 24 h post transfection of siRNA, the cells were mock-treated or treated with 2000 U/mL IFNγ. At 24 h posttreatment, the treated cells were then infected with SARS-CoV-2 at an MOI of 1. The (H) cell lysates and (I) supernatants were harvested at 24 h postinfection for detection of viral genome copy and live infectious virus by RT-qPCR and plaque assays, respectively. $n = 3$. Data are mean ± s.d. from the indicated number of biological repeats. Statistical analyses in panels were performed with (C–F) two-way ANOVA (Sidak's multiple comparisons test), (G) Student's t test and (H and I) one-way ANOVA (Tukey's multiple comparisons test). *$p < 0.05$, **$p < 0.01$, ***$p < 0.001$, and ****$p < 0.0001$. hpi, hours postinfection; ns, not statistically significant.

infectious particle production ($p = 0.0365$) and largely abolished the effect of IFNγ treatment (Figure 6I). Taken together, these results suggest that type-II IFN inhibits SARS-CoV-2 replication in an IDO1-dependent manner.

3.7 | L-Tryptophan (L-Trp) treatment rescues type-II IFN-mediated inhibitory effect on SARS-CoV-2 replication

Previous studies reported that IDO1-mediated nutrient (Trp) depletion (Figure 7A) restricts virus infection by limiting the availability of Trp for viral protein synthesis, such as HIV-1 and HBV.[36,41] We first tested whether IFNγ and IDO1 could modulate endogenous L-Trp expression in Calu3 cells. Our results showed that IFNγ treatment significantly reduced endogenous L-Trp in Calu3 cells, while IDO1 siRNA KD did not increase the L-Trp expression (Figure S8). To evaluate whether Trp can impact IFNγ-mediated restriction of SARS-CoV-2 replication, we treated Calu3 cells with varying concentrations of L-Trp in the presence of IFNγ, followed by SARS-CoV-2. We showed that while IFNγ efficiently inhibited SARS-CoV-2 replication, L-Trp treatment significantly rescued SARS-CoV-2 replication in IFNγ-treated Calu3 cells in a dose-dependent manner (Figure 7B, left panel). Importantly, IFNγ-induced restriction of SARS-CoV-2 was also partially alleviated by the treatment of L-Trp in ex vivo human

lung tissues (Figure 7B, right panel). Overall, these findings suggest that type-II IFN inhibits SARS-CoV-2 replication in both human lung epithelial cells and ex vivo human lung tissues, and that IDO1 significantly contributed to the observed type-II IFN-mediated SARS-CoV-2 inhibition.

4 | DISCUSSION

Type-I and type-III IFNs are potent antiviral cytokines with potent antiviral effects against many viruses, including coronaviruses.[42,43] However, the antiviral activity and mechanism of type-II IFN against SARS-CoV-2 remain largely unexplored. In this study, we comprehensively evaluate the antiviral effects of type-II IFN (IFNγ) on SARS-CoV-2 infection with type-I (IFNβ) and -III IFN (IFNλ1) as controls using human lung epithelial cells (Calu3) and ex vivo human lung tissues. In this study, we demonstrated that IFNγ profoundly inhibited SARS-CoV-2 replication in both human lung epithelial cells and ex vivo human lung tissues. Moreover, IFNγ treatment did not substantially trigger the expression of SARS-CoV-2 entry-related factors and pro-inflammatory responses in ex vivo human lung tissues. Mechanistically, our results revealed that IDO1, which is significantly induced by IFNγ, exerted an inhibitory effect on SARS-CoV-2 as a host restriction factor. Moreover, L-Trp supplementation, a substrate of IDO1, partially restored SARS-CoV-2 replication in
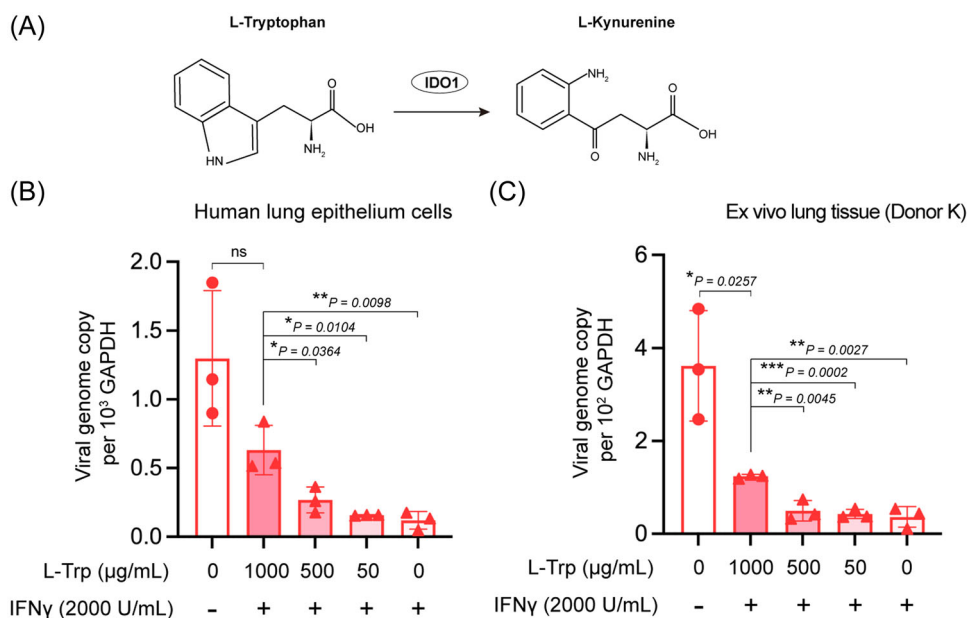

FIGURE 7 L-Tryptophan treatment retrieves SARS-CoV-2 replication in IFNγ-treated Calu3 cells and ex vivo human lung tissues. (A) IDO1-mediated L-Tryptophan (L-Trp) metabolism. (B and C) L-Trp treatment restores the inhibition of SARS-CoV-2 by IFNγ in Calu3 cells and human lung tissues. (B) Calu3 cells and (C) ex vivo human lung tissues were pretreated with L-Trp at the indicated concentrations in the presence of IFNγ (2000 U/mL). After 24 h incubation, the cells were infected with SARS-CoV-2 at an MOI of 0.1 for 2 h; the lung tissues were infected with SARS-CoV-2 viral stock (Viral titer: 10^7 PFU/mL). The cells and lung tissues were then washed with PBS and cultured with medium supplemented with L-Trp and IFNγ accordingly. After 48 h, the cell lysates were harvested for detection of viral genome copy normalized to GAPDH by RT-qPCR. $n = 3$. Data are mean ± s.d. from the indicated number of biological repeats. Statistical analyses were performed with Student's t test and the differences were considered significant when $p < 0.05$. *$p < 0.05$, **$p < 0.01$, and ***$p < 0.001$. ns, not statistically significant.

IFNγ-treated Calu3 cells and ex vivo human lung tissues. Collectively, these findings demonstrate that type-II IFN potently inhibits SARS-CoV-2 replication in human lung epithelial cells and ex vivo human lung tissues through IDO1-mediated antiviral response.

Recent studies have reported the high sensitivity of SARS-CoV-2 to type-I, -II, and -III IFN in multiple models.[8,22,43–45] However, most findings were based on cell lines, which do not completely recapitulate the complexity of human lung infection.[46] Using our established ex vivo human lung tissue culture model,[21,26,47] we hereby demonstrated that IFNγ potently inhibits SARS-CoV-2 replication. Similarly, IFNβ showed antiviral activity in Calu3 cells and ex vivo lung tissues, which is consistent with the observation that type-I IFN is able to inhibit SARS-CoV-2 replication. Previous studies reported that SARS-CoV-2 infection can be controlled by type-III IFN in human intestinal epithelial cells and human airway epithelial cultures.[9,29] Interestingly, we did not observe a potent antiviral effect of type-III IFN on SARS-CoV-2 infection in ex vivo human lung tissues. This inconsistent observation among different studies remains to be dissected and may be related to the different study designs and experimental protocols.

IFNs can play either protective or detrimental roles in the context of viral infections.[48] Exaggerated IFN signaling may result in excessive tissue damage, necrosis, and inflammation, which could contribute to enhanced pathology.[15] In addition, previous studies illustrated that type-I IFN could upregulate the expression of ACE2 expression, which may aggravate SARS-CoV-2 infection.[32,33] Nonetheless, the antiviral activity of IFNs against SARS-CoV-2 infection appears to counterbalance the effects of ACE2 upregulation.[46] In our study, type-II IFN, as well as type-I and -III IFN, did not substantially upregulate pro-inflammatory responses and did not increase the expression of SARS-CoV-2-related entry factors in ex vivo human lung tissues. While IFNγ upregulated a high expression level of IP10 in ex vivo lung tissues, a similar extent of expression level was observed between type-II-treated samples and type-I-treated samples. Since type-I IFNs have been used for the treatment of COVID-19, this evidence may dispel concerns that type-II IFN treatment could enhance disease severity. Importantly, type-II IFN can restrict a variety of viruses in vivo and in vitro, such as HBV, HIV, and Ebola virus (EBOV).[49] Meanwhile, IFNγ plays a protective role on epithelial monolayers from pathogen-mediated injuries.[50] Clinically, type-II IFN (IFN-γ−1b) has been widely used to treat a variety of human diseases, including cancer, fungal infection, and chronic granulomatous disease (CGD).[51] However, a recent study reported that the combination of TNF-α and IFNγ triggers the JAK/STAT1/IRF1 axis, resulting in cytokine-mediated inflammatory cell death.[52,53] These findings suggest that more clinical studies are warranted to fully characterize the safety and efficacy of type-II IFN for clinical use to treat COVID-19.

The antiviral mechanisms of type-II IFN are largely overlapping with that of type-I IFN via similar Janus kinase/signal transducer and activator of transcription (JAK/STAT) protein signal transduction pathways.[11] Type-II IFN binds to IFNGR1 and IFNGR2, which are associated with JAK1 and JAK2, respectively. This leads to phosphorylation of STAT1 and induces the formation of STAT1-STAT1 homodimers that translocate to the nucleus and bind GAS (IFNγ-activated site) elements to initiate the transcription of ISGs.[11] Here, we found that both type-I and -II IFN significantly upregulated the expression of most of the evaluated ISGs in ex vivo human lung tissues. Importantly, IFNγ most robustly upregulated IDO1 expression in ex vivo human lung tissues. IDO1-mediated antiviral activity induced by IFNγ has been shown in the context of multiple virus infections, such as herpes simplex virus and HCV.[40,54] Here, we demonstrated that SARS-CoV-1, ancestral SARS-CoV-2, and SARS-CoV-2 variants (Alpha and Delta) were restricted in an IDO1-dependent manner. Noticeably, IDO1 has substantial negative regulatory effects on inflammation and immunization.[55] In particular, IDO1 plays a critical role in limiting lung inflammation, depletion of IDO1 could exacerbate inflammation of mouse lung.[37,56] These findings suggest that IDO1-mediated response not only restricts virus infection but may also contribute to attenuating the inflammation and lung damage during SARS-CoV-2 infection. Previous studies demonstrated that IDO1-induced nutrient (L-Trp) depletion contributed to antiviral activity of IFNγ against virus infection, such as measles virus, HBV, and HIV.[36,41,57] L-Trp, the substrate of IDO1, is required for nascent viral protein synthesis. In the present study, L-Trp supplementation partly restored IFNγ-inhibited SARS-CoV-2 replication in both human lung epithelial cells and ex vivo human lung tissues, suggesting that the depletion of L-Trp contributes to IDO-mediated antiviral effect on SARS-CoV-2. These findings provide novel insights into the potential anti-SARS-CoV-2 strategy with nutrient-depletion. In summary, our study provides insights into IFNγ and IDO1-mediated pathways as potential intervention strategies against SARS-CoV-2 and other viruses.

AUTHOR CONTRIBUTIONS

Study design: Dong Yang and Hin Chu. *Supervision*: Hin Chu. *Performed experiments*: Dong Yang, Chaemin Yoon, Tsz-Yat Luk, Huiping Shuai, Yuxin Hou, Xiner Huang, Bingjie Hu, Yue Chai, Terrence Tsz-Tai Yuen, Yuanchen Liu, Tianrenzheng Zhu, Huan Liu, Jialu Shi, Yang Wang, LC, Yuxin Hou, Anna Jinxia Zhang, Shuofeng Yuan, Bao-Zhong Zhang, Hin Chu. *Data analysis*: Dong Yang, Chaemin Yoon, Jasper Fuk-Woo Chan, Yao-Wei Huang. and Hin Chu. *Visualization*: Dong Yang, Chaemin Yoon, and Hin Chu. *Writing—original draft*: Dong Yang and Hin Chu. *Writing—review & editing*: Dong Yang, Jasper Fuk-Woo Chan, and Hin Chu. *Provided key resources and/or funding*: Hin Chu.

ACKNOWLEDGMENTS

CONFLICTS OF INTEREST STATEMENT

J. F.-W. C. has received travel grants from Pfizer Corporation Hong Kong and Astellas Pharma Hong Kong Corporation Limited and was an invited speaker for Gilead Sciences Hong Kong Limited and Luminex Corporation. The remaining authors declare no conflict of interest.

DATA AVAILABILITY STATEMENT

All data needed to evaluate the conclusions in the paper are present in the paper and the Supporting Information.

ORCID

Jasper Fuk-Woo Chan https://orcid.org/0000-0001-6336-6657
Xiner Huang http://orcid.org/0000-0002-0154-8372
Shuofeng Yuan https://orcid.org/0000-0001-7996-1119

REFERENCES

1. WHO. Coronavirus Disease (COVID-19) Weekly Epidemiological. WHO; 2022:85. https://www.who.int/publications/m/item/weekly-epidemiological-update-on-covid-19—29-march-2022
2. Liu L, Iketani S, Guo Y, et al. Striking antibody evasion manifested by the Omicron variant of SARS-CoV-2. Nature. 2022;602(7898):676-681.
3. Shuai H, Chan JFW, Hu B, et al. Attenuated replication and pathogenicity of SARS-CoV-2 B.1.1.529 Omicron. Nature. 2022;603(7902):693-699.
4. Shuai H, Chan JFW, Hu B, et al. The viral fitness and intrinsic pathogenicity of dominant SARS-CoV-2 Omicron sublineages BA.1, BA.2, and BA.5. EBioMedicine. 2023;95:104753.
5. Chan JFW, Hu B, Chai Y, et al. Virological features and pathogenicity of SARS-CoV-2 Omicron BA.2. Cell Rep Med. 2022;3(9):100743.
6. Iketani S, Liu L, Guo Y, et al. Antibody evasion properties of SARS-CoV-2 Omicron sublineages. Nature. 2022;604(7906):553-556.
7. Hu B, Chan JFW, Liu Y, et al. Divergent trajectory of replication and intrinsic pathogenicity of SARS-CoV-2 Omicron post-BA.2/5 subvariants in the upper and lower respiratory tract. EBioMedicine. 2024;99:104916.
8. Mantlo E, Bukreyeva N, Maruyama J, Paessler S, Huang C. Antiviral activities of type I interferons to SARS-CoV-2 infection. Antiviral Res. 2020;179:104811.
9. Stanifer ML, Kee C, Cortese M, et al. Critical role of type III interferon in controlling SARS-CoV-2 infection in human intestinal epithelial cells. Cell Rep. 2020;32(1):107863.
10. Vanderheiden A, Ralfs P, Chirkova T, et al. Type I and type III interferons restrict SARS-CoV-2 infection of human airway epithelial cultures. J Virol. 2020;94(19):e00985-20.
11. Platanias LC. Mechanisms of type-I- and type-II-interferon-mediated signalling. Nat Rev Immunol. 2005;5(5):375-386.
12. McNab F, Mayer-Barber K, Sher A, Wack A, O'Garra A. Type I interferons in infectious disease. Nat Rev Immunol. 2015;15(2):87-103.
13. Sen GC. Viruses and interferons. Annu Rev Microbiol. 2001;55:255-281.
14. Lazear HM, Schoggins JW, Diamond MS. Shared and distinct functions of type I and type III interferons. Immunity. 2019;50(4):907-923.
15. Park A, Iwasaki A. Type I and type III interferons - induction, signaling, evasion, and application to combat COVID-19. Cell Host Microbe. 2020;27(6):870-878.
16. Hung IF-N, Lung K-C, Tso EY-K, et al. Triple combination of interferon beta-1b, lopinavir–ritonavir, and ribavirin in the treatment of patients admitted to hospital with COVID-19: an open-label, randomised, phase 2 trial. Lancet. 2020;395:1695-1704.
17. NIH U. Coronavirus Disease 2019 (COVID-19) Treatment Guidelines. NIH U; 2020.
18. Miorin L, Kehrer T, Sanchez-Aparicio MT, et al. SARS-CoV-2 Orf6 hijacks Nup98 to block STAT nuclear import and antagonize interferon signaling. Proc Natl Acad Sci. 2020;117(45):28344-28354.
19. Yang D, Chu H, Hou Y, et al. Attenuated interferon and proinflammatory response in SARS-CoV-2-infected human dendritic cells is associated with viral antagonism of STAT1 phosphorylation. J Infect Dis. 2020;222(5):734-745.
20. Busnadiego I, Fernbach S, Pohl MO, et al. Antiviral activity of type I, II, and III interferons counterbalances ACE2 inducibility and restricts SARS-CoV-2. mBio. 2020;11(5):e01928-20.
21. Chu H, Chan JFW, Wang Y, et al. Comparative replication and immune activation profiles of SARS-CoV-2 and SARS-CoV in human lungs: an ex vivo study with implications for the pathogenesis of COVID-19. Clin Infect Dis. 2020;71(6):1400-1409.
22. Shuai H, Chu H, Hou Y, et al. Differential immune activation profile of SARS-CoV-2 and SARS-CoV infection in human lung and intestinal cells: implications for treatment with IFN-beta and IFN inducer. J Infect. 2020;81(4):e1-e10.
23. Chu H, Chan JFW, Yuen TTT, et al. Comparative tropism, replication kinetics, and cell damage profiling of SARS-CoV-2 and SARS-CoV with implications for clinical manifestations, transmissibility, and laboratory studies of COVID-19: an observational study. Lancet Microbe. 2020;1(1):e14-e23.
24. Shuai H, Chan JFW, Yuen TTT, et al. Emerging SARS-CoV-2 variants expand species tropism to murines. EBioMedicine. 2021;73:103643.
25. Chan JFW, Huang X, Hu B, et al. Altered host protease determinants for SARS-CoV-2 Omicron. Sci Adv. 2023;9(3):eadd3867.

26. Chu H, Hou Y, Yang D, et al. Coronaviruses exploit a host cysteine-aspartic protease for replication. *Nature*. 2022;609(7928):785-792.

27. Chu H, Shuai H, Hou Y, et al. Targeting highly pathogenic coronavirus-induced apoptosis reduces viral pathogenesis and disease severity. *Sci Adv*. 2021;7(25):eabf8577.

28. Chan JFW, Yip CCY, To KKW, et al. Improved molecular diagnosis of COVID-19 by the novel, highly sensitive and specific COVID-19-RdRp/Hel real-time reverse transcription-PCR assay validated in vitro and with clinical specimens. *J Clin Microbiol*. 2020; 58(5):e00310-20.

29. Felgenhauer U, Schoen A, Gad HH, et al. Inhibition of SARS-CoV-2 by type I and type III interferons. *J Biol Chem*. 2020;295(41): 13958-13964.

30. Yang D, Chu H, Lu G, et al. STAT2-dependent restriction of Zika virus by human macrophages but not dendritic cells. *Emerg Microbes Infect*. 2021;10:1-42.

31. Huang C, Wang Y, Li X, et al. Clinical features of patients infected with 2019 novel coronavirus in Wuhan, China. *Lancet*. 2020; 395(10223):497-506.

32. Hou YJ, Okuda K, Edwards CE, et al. SARS-CoV-2 reverse genetics reveals a variable infection gradient in the respiratory tract. *Cell*. 2020;182(2):429-446.e14.

33. Onabajo OO, Banday AR, Stanifer ML, et al. Interferons and viruses induce a novel truncated ACE2 isoform and not the full-length SARS-CoV-2 receptor. *Nature Genet*. 2020;52(12):1283-1293.

34. Diamond MS, Farzan M. The broad-spectrum antiviral functions of IFIT and IFITM proteins. *Nat Rev Immunol*. 2013;13(1):46-57.

35. Schoggins JW, Rice CM. Interferon-stimulated genes and their antiviral effector functions. *Curr Opin Virol*. 2011;1(6):519-525.

36. Mao R, Zhang J, Jiang D, et al. Indoleamine 2,3-dioxygenase mediates the antiviral effect of gamma interferon against hepatitis B virus in human hepatocyte-derived cells. *J Virol*. 2011;85(2): 1048-1057.

37. Thomas T, Stefanoni D, Reisz JA, et al. COVID-19 infection alters kynurenine and fatty acid metabolism, correlating with IL-6 levels and renal status. *JCI Insight*. 2020;5(14):e140327.

38. Hornyák L, Dobos N, Koncz G, et al. The role of indoleamine-2,3-dioxygenase in cancer development, diagnostics, and therapy. *Front Immunol*. 2018;9:151.

39. Desai N, Neyaz A, Szabolcs A, et al. Temporal and spatial heterogeneity of host response to SARS-CoV-2 pulmonary infection. *Nat Commun*. 2020;11(1):6319.

40. Adams O, Besken K, Oberdörfer C, MacKenzie CR, Rüßing D, Däubener W. Inhibition of human herpes simplex virus type 2 by interferon γ and tumor necrosis factor α is mediated by indoleamine 2,3-dioxygenase. *Microb Infect*. 2004;6(9):806-812.

41. Kane M, Zang TM, Rihn SJ, et al. Identification of interferon-stimulated genes with antiretroviral activity. *Cell Host Microbe*. 2016;20(3):392-405.

42. Chan JFW, Chan KH, Kao RYT, et al. Broad-spectrum antivirals for the emerging Middle East respiratory syndrome coronavirus. *J Infect*. 2013;67(6):606-616.

43. Yuan S, Chan CCY, Chik KKH, et al. Broad-spectrum host-based antivirals targeting the interferon and lipogenesis pathways as potential treatment options for the pandemic coronavirus disease 2019 (COVID-19). *Viruses*. 2020;12(6):628.

44. Winstone H, Lista MJ, Reid AC, et al. The polybasic cleavage site in SARS-CoV-2 spike modulates viral sensitivity to type I interferon and IFITM2. *J Virol*. 2021;95(9):e02422-20.

45. Nchioua R, Kmiec D, Müller JA, et al. SARS-CoV-2 is restricted by zinc finger antiviral protein despite preadaptation to the low-CpG environment in humans. *mBio*. 2020;11(5):e01930-20.

46. Schaller MA, Sharma Y, Dupee Z, et al. Ex vivo SARS-CoV-2 infection of human lung reveals heterogeneous host defense and therapeutic responses. *JCI Insight*. 2021;6(18):e148003.

47. Chu H, Hu B, Huang X, et al. Host and viral determinants for efficient SARS-CoV-2 infection of the human lung. *Nat Commun*. 2021;12(1): 134.

48. Stifter SA, Feng CG. Interfering with immunity: detrimental role of type I IFNs during infection. *J Immunol*. 2015;194(6):2455-2465.

49. Kang S, Brown HM, Hwang S. Direct antiviral mechanisms of interferon-gamma. *Immune Netw*. 2018;18(5):e33.

50. Kak G, Raza M, Tiwari BK. Interferon-gamma (IFN-γ): exploring its implications in infectious diseases. *Biomol Concepts*. 2018;9(1):64-79.

51. Friedman RM. Clinical uses of interferons. *Br J Clin Pharmacol*. 2008;65(2):158-162.

52. Karki R, Sharma BR, Tuladhar S, et al. Synergism of TNF-α and IFN-γ triggers inflammatory cell death, tissue damage, and mortality in SARS-CoV-2 infection and cytokine shock syndromes. *Cell*. 2021;184(1):149-168.

53. Tan Y, Tang F. SARS-CoV-2-mediated immune system activation and potential application in immunotherapy. *Med Res Rev*. 2021;41(2):1167-1194.

54. Frese M, Schwärzle V, Barth K, et al. Interferon-γ inhibits replication of subgenomic and genomic hepatitis C virus RNAs: interferon-γ inhibits replication of subgenomic and genomic hepatitis C virus RNAs. *Hepatology*. 2002;35(3):694-703.

55. Wu H, Gong J, Liu Y. Indoleamine 2, 3-dioxygenase regulation of immune response (review). *Mol Med Rep*. 2018;17(4):4867-4873.

56. Lee SM, Park HY, Suh YS, et al. Inhibition of acute lethal pulmonary inflammation by the IDO-AhR pathway. *Proc Natl Acad Sci*. 2017;114(29):E5881-E5890.

57. Obojes K, Andres O, Kim KS, Däubener W, Schneider-Schaulies J. Indoleamine 2,3-dioxygenase mediates cell type-specific anti-measles virus activity of gamma interferon. *J Virol*. 2005;79(12): 7768-7776.

SUPPORTING INFORMATION

Additional supporting information can be found online in the Supporting Information section at the end of this article.